Observing Nightlights from Space with TEMPO

James Carr[1,*], Xiong Liu[2], Brian Baker[3], Kelly Chance[2]

[1]Carr Astronautics Corp., Greenbelt, MD, USA
[2]Harvard-Smithsonian Center for Astrophysics, Cambridge, MA, USA
[3]Ball Aerospace and Technologies Corp., Boulder, CO, USA

Received 05 December 2016, Accepted 08 February 2017

Abstract

The Tropospheric Emissions: Monitoring of Pollution (TEMPO) instrument is a NASA Earth Venture Instrument set to fly in the 2018-2021 timeframe and cover North America from a geostationary orbit. TEMPO is a powerful spectrometer sampling UV and visible wavelengths in two channels (290-490 nm and 540-740 nm) in 0.2 nm steps. This spectroscopic capability will enable TEMPO to characterize many types of artificial lighting at night in addition to its regular daytime air quality and atmospheric chemistry mission. This paper describes the TEMPO instrument and our planned approach to make nighttime observations. A spectral retrieval algorithm will estimate the contributions from sources in a spectral library to map out the usage of various types of lighting (e.g., Hg vapor, high and low pressure Na vapor, LED, fluorescent, and incandescent) over North America. We calculate the sensitivities of such nightlight retrievals using the measured properties of our flight detectors and optics, and conclude that TEMPO will complement well the VIIRS Day-Night Band for the study of artificial lighting at night from space by offering a new and powerful capability to discriminate between lighting types.

Keywords: Nightlights, Spectroscopy, VIIRS day-night band

1. Introduction

The Tropospheric Emissions: Monitoring of Pollution (TEMPO) instrument [1] is supported by the NASA Earth Venture Instrument (EV-I) program. It will fly as a hosted payload on a geostationary commercial communications satellite sometime between 2018 and 2021 depending on available flight opportunities. TEMPO will cover all the United States except for Alaska and Hawaii, Mexico as far south as Mexico City, Canada as far north as the Alberta oil sands, and much of the Caribbean. This entire area will be covered once per hour with the possibility of more rapidly revisiting smaller subareas. TEMPO collects and spectrally disperses reflected sunlight to reveal the presence of various trace gas species through their distinctive absorption spectra. Its primary mission is to monitor air quality and study the chemistry of trace gases in the atmosphere and support the study of aerosols, clouds, and chlorophyll fluorescence. TEMPO will be capable of producing vertical column densities of various gas species, including O3, NO2, SO2, H2CO, C2H2O2, BrO, IO, and H2O as well as ozone profiles including tropospheric ozone on an hourly basis. The primary mission of TEMPO is conducted only during daylight hours, which leaves TEMPO available at night for the spectroscopic observation of nightlights, which is the subject of this paper. Artificial lighting is a marker for human economic activity with implications for energy efficiency, darkness of the nighttime sky, and ecological impacts on both humans and other lifeforms. These implications are explored as part of the Artificial Lighting at Night (ALAN) conference series and this

* Carr J, *E-mail address:* jcarr@carrastro.com

paper is based on our presentation at ALAN 2016. For a review of nightlights imagery sources and several research application areas with a good bibliography, see Kyba et. al. [2].

Interest in the observation of nightlights from space has grown since the launch of the Visible Infrared Imaging Radiometer Suite (VIIRS) with its Day-Night Band (DNB) on the Suomi National Polar-orbiting Partnership spacecraft in 2011. The VIIRS-DNB represents a significant improvement [3] in capability relative to the legacy Operational Linescan System (OLS) flown on Defense Meteorological Satellite Program (DMSP) spacecraft since 1972 (for a good review of research applications using OLS nighttime imagery conducted over the years, see Huang et. al. [4]). The VIIRS-DNB capabilities for worldwide mapping of light pollution were recently featured by the publication of an atlas of night sky quality [5] that updates a similar atlas produced from OLS data in 2001 [6]. However, the nightlight sensing capability of VIIRS is monochromatic leaving it unable to distinguish between different types of artificial lighting. It is known that the spectral characteristics of artificial lights are important. For example, blue light is scattered more strongly in the atmosphere (Rayleigh scattering) than red light and therefore blue light contributes more to the brightening of the night sky than red light, which is the same reason that scattered sun light makes the sky appear blue. A second example is the impact on human health through the mechanism of melatonin suppression in response to exposure to primarily blue light. Concern over the disruption of circadian rhythms from artificial lighting at night and its impact on human health including elevated cancer risks prompted the American Medical Association to issue a policy statement on light pollution in 2012 [7]. As Light Emitting Diode (LED) luminaires become more prevalent in outdoor lighting, the spectral characteristics of nightlights will be changing too, with typically more light being emitted in the bluer wavelengths, which is a concern relative to both the examples just cited. The VIIRS-DNB, with a lower wavelength cutoff at 500 nm, is also less well suited to observing LED lighting that emits a significant fraction of its light in bluer wavelength regimes.

Multispectral and hyperspectral nighttime imagery is therefore desirable to aid in the analysis of nighttime lighting patterns and particularly the adoption of LED technology. A collection of nighttime multispectral images of cities is presently available to researchers from an astronaut photography program conducted from the International Space Station (ISS). An atlas exists to facilitate accessing these photographs from an even larger collection in the NASA gateway for astronaut photography [8]. These photographs have been used to provide insight into changes in lighting of some European cities where patterns of illumination have been observed over time of night and year to year and lighting types in use have been identified by their color [2]. We anticipate that TEMPO and possibly some other spectrometers that we discuss in Section 5 should provide additional capabilities to more richly describe the artificial lighting of our planet at night.

2. TEMPO Instrument and Data

Fig. 1 shows the components of the TEMPO instrument. Light enters through the calibration mechanism, which can be open for collecting Earth data, closed for safety, or have either one of two diffuser plates inserted into the optical path for calibration using the sun as a source. A scan mechanism moves a flat scan mirror that allows the TEMPO field of view to be scanned across the Earth from east to west during collection of a scan. A full scan nominally consists of 1282 scan steps in about one hour. At each scan step, light reflected off the scan mirror is projected by a three-mirror telescope onto the entrance slit of an Offner-type spectrometer where it is spectrally dispersed onto two Charged Coupled Device (CCD) focal plane arrays nominally operated at -20°C to reduce dark current. Each CCD records the spectra of ~2038 spatial pixels arranged north to south in ~1001 spectral bins, with exact numbers to be known after final assembly of the spectrometer. One CCD covers the spectral range from 290 nm to 490 nm (UV to blue) in 0.2 nm steps and the other CCD covers the spectral range from 540 nm to 740 nm (green to red) also in 0.2 nm steps. The size of the spectral gap between 490 nm and 540 nm is dictated by the number of spectral pixels on the CCDs, the physical restrictions on the devices as to how closely they can be spaced, as well as the needs of the scientific community to adequately cover ozone absorption in the visible for lower tropospheric ozone retrievals and extend the spectral range to 740 nm for vegetation products using chlorophyll fluorescence. The intrinsic spectral resolution of the TEMPO spectrometer is 0.6 nm (full width at half maximum).

The focal plane has a read-while-integrating architecture, with the flexibility to specify the desired integration time per frame and number of co-added frames. We co-add frames for daylight observations to avoid having the CCD wells overfill while achieving a dwell time per spatial pixel equal to the integration time times the number

of co-adds. Overfilling is not a concern for nightlights observations, so we will take advantage of the operational flexibility of TEMPO to program it to integrate longer than nominally planned for daylight observations and co-add fewer frames. Reducing co-adds saves on read noise from the readout circuitry. The dominant noise sources for nightlights observations are Poisson noise, mostly from the dark current background, and read noise. We analyze the sensitivity of TEMPO for nightlights observations using the measured characteristics of its flight parts, including CCD dark currents and quantum efficiencies and the efficiency of the spectrometer grating. Dark current will gradually increase in flight with the total ionizing dose of radiation, resulting in best performance at the beginning of life and graceful degradation thereafter.

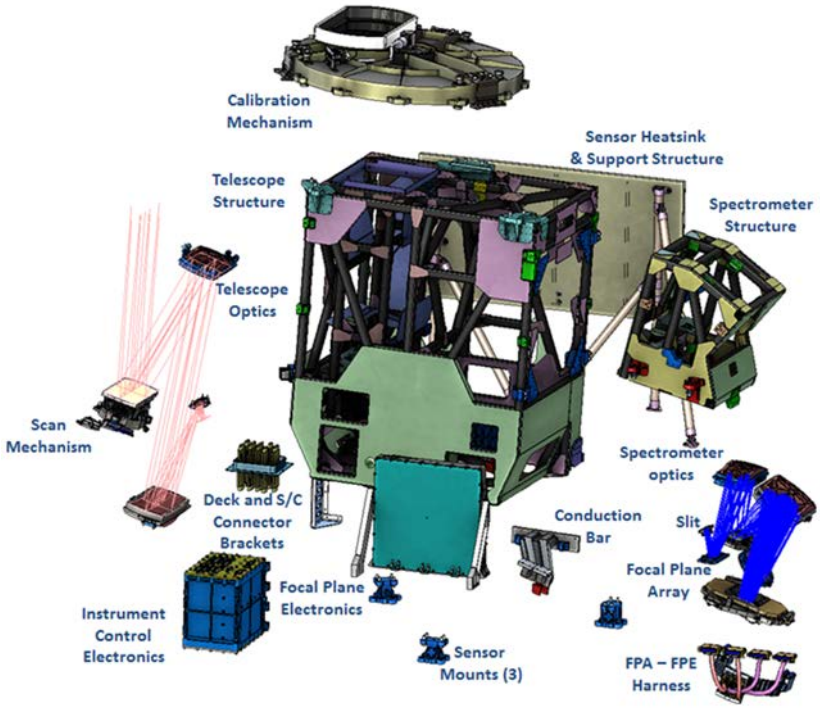

Fig. 1. Components of the TEMPO Instrument are shown in an exploded view. The optical system comprises a calibration mechanism, a scan mechanism, a three-mirror telescope, and a grating spectrometer. Instrument control electronics and thermal control surfaces will be integrated alongside TEMPO on the nadir facing deck of a commercial communications satellite. The cant angles for TEMPO to orient it towards the desired field of regard will be known once its exact longitude station has been determined after host spacecraft selection.

A nominal full-scan level 1b product is a data "cube" of 1282 (spatial) x 2038 (spatial) x 2002 (spectral) voxels. Each voxel holds a calibrated spectral radiance value and each spatial plane within the data cube has a nominal wavelength assignment; however, there is a small spectral cross-coupling between the two axes of the CCDs, so calibrated wavelengths are included as metadata in the product to more precisely mark the spectral content of voxels. Each spatial pixel has an instantaneous field of view equal to approximately 120 □rad (East-West) x 41.8 □rad (North-South), which corresponds to a footprint on the ground of 4.4 km x 2.1 km at the center of the field of regard (34.45°N, 94.72°W) when TEMPO is stationed at 100°W longitude above the Equator. No remapping or resampling is performed on the spatial pixels to compensate for spacecraft motion, scanner errors, or other geometric distortions, but metadata is provided in the product to accurately geolocate each spatial pixel. The footprint of a spatial pixel on the ground will grow in area as the limb is approached introducing effectively more spatial averaging of sources within it. Scanning across the field of regard is nominally in equal angle steps and there is no compensation for the growth of the area of spatial pixels moving further off nadir as is done with VIIRS. In addition, TEMPO will collect dark images when the calibration mechanism is closed before and after nominal Earth viewing, and TEMPO will collect solar calibration images using one of two transmissive diffusers once a day. One diffuser is for daily use and the other is a reference diffuser to be used once every few months to track

any change in the diffuser that is used daily. The solar calibration images will help to trend instrument response over time and will be utilized to track CCD performance in the way a typical flat-field image is used.

TEMPO data, including radiometrically calibrated and geographically located level 1b radiances and higher level products, will be first released to the public 4-6 months after the beginning of routine operations. Thereafter, level 1b data will be available within ~3 hours of observation through the Smithsonian Astrophysical Observatory (SAO) website, kept online for 30 days, and then permanently archived at NASA's Atmospheric Science Data Center for public distribution.

3. Plan for Nighttime Observing

Nightlights observing will be conducted when TEMPO is not performing its primary air quality and atmospheric chemistry mission. However, there is an important safety constraint because the TEMPO spectrometer entrance slit can be damaged if intense sunlight impinges on it. To avoid this, we do not open the TEMPO aperture door whenever the sun is within 60° of the optical axis. This still leaves plenty of opportunities to collect nightlights data, particularly in the northern hemisphere winter, as shown in Fig. 2 where solar illumination is depicted for three major metropolitan areas from the east to the west across the field of regard as a function of U.S. Central Standard Time (CST) and season (declination of the sun above the Equator). Nightlights observations over the East Coast and Midwestern U.S. can be conducted prior to midnight CST and over the West Coast after midnight CST. The aperture door will need to be shut for up to eight hours roughly centered around midnight CST. Although in principle we could reopen the aperture door during the umbra of the eclipse of the sun by the Earth, we are unlikely to do so because of the risk of not being able to close the aperture in time.

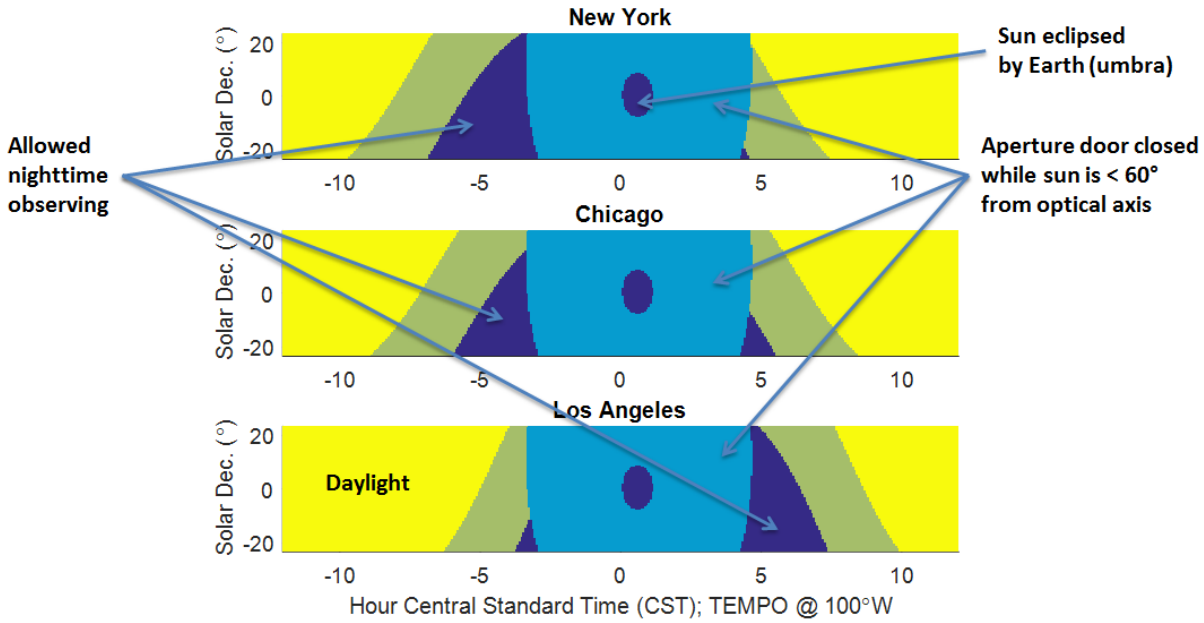

Fig. 2. Nighttime observing with TEMPO depends on the season (solar declination), time of day, and location. Daylight observing times when the solar zenith angle is less than 80° are indicated by the yellow fill and nighttime observing times when the solar zenith angle is greater than 108° (astronomical night) are indicated by the dark blue fill. The aperture door will be shut for safety when the sun is within 60° of the optical axis (light blue). The most desirable longitude for TEMPO is 100°W, which puts it in the U.S. Central Time zone with Chicago and observing over eastern cities such as New York naturally would occur earlier and observing over western cities such as Los Angeles later.

We intend to dwell for about 10 seconds per spatial pixel, about four times longer than dwells for daylight collections, which means that TEMPO will cover the field of regard about four times more slowly as well. It will take roughly two hours to cover the eastern half and two hours to cover the western half of the field of regard and

we may collect the full field of regard piecemeal over several nights. A dark signal calibration is planned before beginning nightlights observing and again to verify the dark calibration at the completion of observing. The dark calibration will consist of 16 dwells of about 10 seconds each with the aperture door shut that will then be averaged together to estimate the dark signal. Because of hardware limitations on the maximum integration time for a frame, we will co-add two frames each integrated for five seconds to form our dwells. A solar calibration is performed daily, regardless of whether we are conducting nightlights observations, with one of the diffuser plates in place to attenuate and diffuse incoming sunlight. This activity is performed when the sun is 30° from the optical axis. Since 30° is within our exclusion zone, there is no conflict between the two calibration activities or nightlights observations.

4. Nightlights Retrievals

4.1. Spectral Library

The fine spectral resolution offered by TEMPO enables light from various types of known sources to be identified by origin. The NOAA National Geophysical Data Center (NGDC) has made publicly available many examples of spectra for various categories of sources [9-10]. These spectra form the initial basis set for our retrieval algorithm that assigns the light from each spatial pixel to a linear combination of sources in accordance with the strength of each source.

Fig. 3 shows the spectra of ten different lighting types to be used as a basis set for spectral fitting in our retrieval analysis. Each spectrum, $r_p(\lambda)$, has been normalized so that if the entire signal in a spatial pixel were to be of type p then it would produce a response in the VIIRS Day-Night Band (DNB) equal to 1 nW sr-1 cm -2. We will say that such a source has strength equal to 1 DNB unit. The NGDC spectra are not published for wavelengths shorter than 350 nm, so we do not use the TEMPO wavelength bins from 290-350 nm in our retrieval analysis.

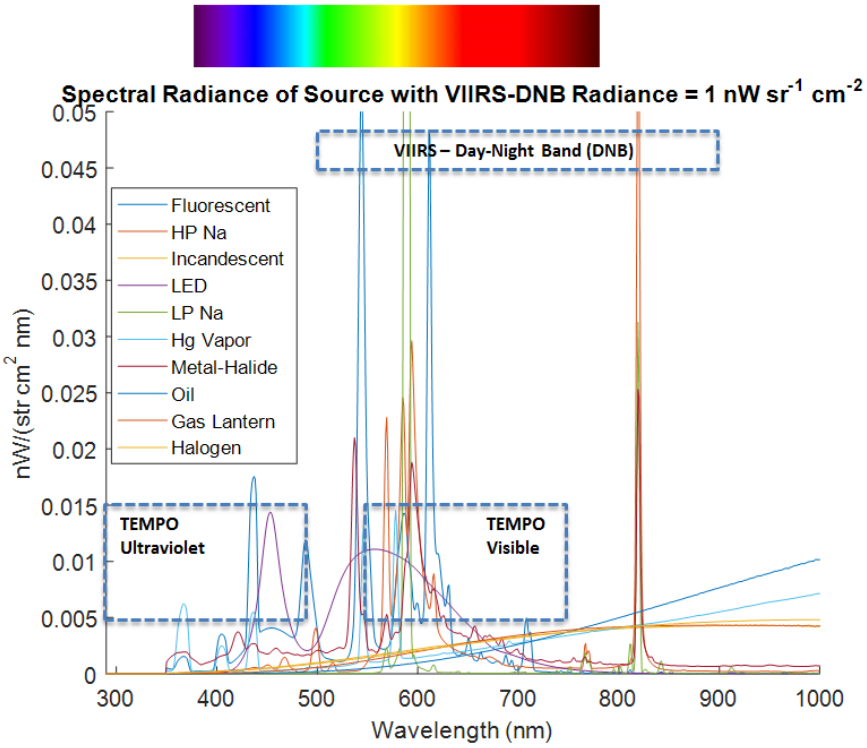

Fig. 3. A spectral library from NOAA National Geophysical Data Center (NGDC) will be used to retrieve the strengths of contributing sources. Each basis function in the library is normalized so that it would produce a signal in the VIIRS-DNB of 1 nW sr-1 cm -2. The spectral passband of the VIIRS-DNB is indicated by the dashed box. The passbands for each TEMPO CCD are similarly indicated, but unlike for VIIRS, each is subdivided into ~1000 spectral planes. The data plotted from NGDC has not been convolved with the spectral line response function of the TEMPO spectrometer and has been sampled at in 1 nm steps, which is coarser than the spectral resolution of TEMPO.

The gap in the spectral coverage of TEMPO is not a significant handicap relative to the sources cataloged by NGDC as most spectral features are covered by one of the two TEMPO bands.

4.2. Retrieval Sensitivity

The nightlights signal level for a voxel is the number of photoelectrons accumulated during the dwell minus the calibrated dark signal photoelectrons. We model the nightlights signal to be a linear combination of sources in our spectral library. Let $\bar{r}_p(\lambda_k)$ be the spectral radiance of source type p from our spectral library after being convolved with the spectral line response function of the spectrometer for a spectral bin centered at the wavelength λ_k (if the index p is not explicitly written, the symbol should be understood to be a vector with components in the space of sources). The radiance in the spectral bin k is represented as a superposition $\bar{r}(\lambda_k) \cdot \alpha$, where the dot notation indicates a summation over all source types p. For a spatial pixel (i,j), the modeled signal level in a voxel is $H(\lambda_k) \cdot \alpha_{i,j}$, where $H_p(\lambda_k) = G_k \bar{r}_p(\lambda_k)$ and G_k is the conversion factor from radiance to photoelectrons involving the quantum efficiency of the CCD and the transmission of the optical system. The retrieved strengths for each spatial pixel form a vector $\hat{\alpha}_{i,j}$ that best fits the signal. In a weighted linear least-squares analysis, the uncertainty in the retrieved strengths is described by a covariance matrix:

$$cov(\hat{\alpha}_{i,j}) = \left(H^T R_i(\alpha_{i,j})^{-1} diag(m_i) H\right)^{-1}. \quad (1)$$

The matrix H has as many columns as α and as many rows as there are spectral bins. The matrix $R_i(\alpha)$ is a noise covariance matrix for the measured signal level in each spectral bin for a given CCD spatial row i. A small number of CCD pixels (<0.1%) have significantly higher than average dark current, or their response is not representative of the majority of CCD pixels. In this case, those pixels are designated as "inoperable" and the mask $m_{i,k}$ is set to zero for inoperable pixels, and one otherwise. R_i is assumed to be diagonal since the noise in each CCD pixel is expected to be independent. It has dark current and readout noise contributions from both the Earth scene and the dark signal calibration. In principle, there is a Poisson noise contribution from the nightlights signal itself; however, in a sensitivity analysis, we are looking for the lowest detectable signals and therefore, we consider the noise in the limit $\alpha \longrightarrow 0$, when:

$$R_i = diag\left((1 + 1/N_{dark}) N_{add} (D_i + \sigma_{ro}^2)\right). \quad (2)$$

The dominant noise contribution comes from Poisson noise in each co-added frame (N_{add}, nominally 2), which has a variance equal to the dark signal $D_{i,k}$ for spatial row i and spectral column k of the CCD, and is proportional to the frame integration time. The readout noise variance σ_{ro}^2 will be typically smaller and is applied to each co-added frame. Both Poisson noise from the dark signal and readout noise affect the signal from the Earth scene and the dark signal calibration; however, the variance from the dark signal calibration is reduced by averaging N_{dark} (nominally 16) frames during the dark signal calibration.

Using our measurements from the flight parts, we can calculate the retrieval sensitivity for each type of lighting. The square-roots of the diagonal components of the covariance matrix in Equation (1) are these sensitivities (i.e., the one-sigma error on zero signal). Note that since the spectral library basis functions are normalized to a unit response in the VIIRS-DNB, the uncertainties are calculated in DNB units. These sensitivities are plotted in Fig. 4 for retrievals using TEMPO alone. Our spectrometer is very good at detecting lighting types with very sharp spectral features, but less sensitive to thermal sources, such as incandescent lamps and not as adept at discriminating between subtypes of such sources. For Fig. 4, we have aggregated all thermal sources into a single type for retrieving the strengths of the various lighting types. VIIRS-DNB, on the other hand, has a broad spectral bandwidth and is quite good at detecting lighting of all types, but incapable of discrimination between types. By fusing data from TEMPO and VIIRS-DNB, we can improve our retrieval sensitivity, especially for thermal

sources. We do this by remapping a VIIRS-DNB image or composite image into the TEMPO geometry, binning it into the TEMPO spatial resolution, and then considering the remapped and binned VIIRS-DNB pixels to be samples of an additional spectral plane in our retrieval. The resulting covariance for the retrieved strengths is

$$cov(\hat{\alpha}_{i,j}) = \left(H^T R_i(\alpha_{i,j})^{-1} diag(m_i) H + H_{DNB}^T R_{DNB}^{-1} H_{DNB}\right)^{-1}. \quad (3)$$

Here, R_{DNB} is the radiometric noise covariance in the binned VIIRS-DNB pixels. We can estimate that from the VIIRS-DNB radiometric noise at its native resolution and adjust for the fact that there will be approximately 16 VIIRS-DNB pixels binned within each TEMPO pixel. VIIRS-DNB radiometric noise is lower than its specified value for the Suomi-NPP satellite, but for conservatism we should assume only specified performance, which is a signal-to-noise ratio of 6:1 at a signal of 3 DNB units or 0.5 DNB units [11]. The binning will reduce the noise variance by a factor of 1/16, so we can estimate $R_{DNB} = (0.5\ DNB)^2/16$. The matrix H_{DNB} has as many rows as basis functions but only a single column. It is in fact a column vector of all ones since the basis functions have been normalized to a response in the VIIRS-DNB of one DNB unit. Fig. 4 also shows sensitivities for retrievals using both TEMPO and VIIRS data. We see significant improvement with the retrieval of incandescent lighting and marginal improvement elsewhere. Simultaneity between TEMPO scans and VIIRS overpasses will not be assured but we can at least use NGDC monthly clear sky composites to fuse with our TEMPO data after the fact and Geostationary Operational Environmental Satellite (GOES) cloud products to indicate when spatial pixels are cloud contaminated. To deal with transient variations in lighting usage will require more contemporaneous VIIRS-DNB data.

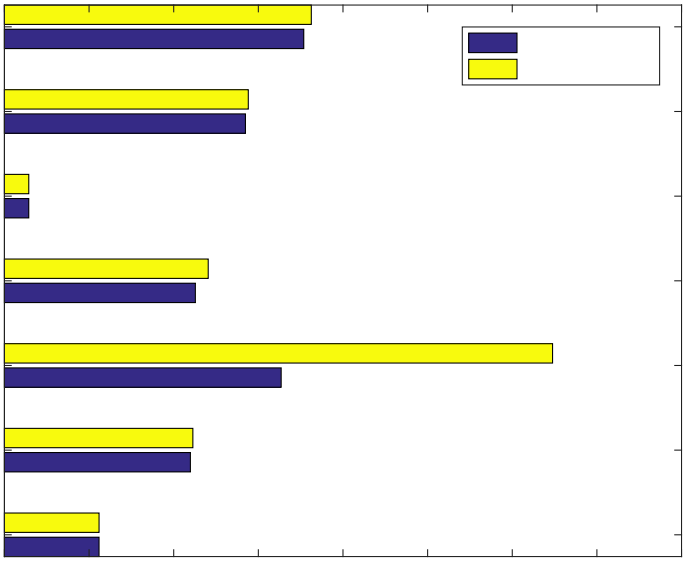

Fig. 4. Retrieval sensitivities are calculated for seven classes of sources in units of equivalent response in the VIIRS-DNB (1 DNB is equivalent to a radiance of 1 nW sr-1 cm -2 in the DNB passband). Each sensitivity is the minimum detectable signal of that type as defined by a signal-to-noise ratio of one.

4.3. Background Sources of Light

The prior analysis looked at the problem of retrieval sensitivity only in the presence of instrumental noise. Natural sources of illumination will exist that may impact the retrievals of light from anthropogenic sources and are interesting on their own, including backgrounds due to moonlight, starlight, and zodiacal light, lightning, auroras, and airglow. Normally, we do not consider these backgrounds in our daytime retrievals. They will induce a retrieval signal to the extent that their spectra are correlated with the spectra in our source library. We know from VIIRS that such backgrounds can be observed [12]. Moonlit scenes should present the brightest

backgrounds and can have responses in the VIIRS-DNB >10 DNB units. Moonlight exhibits a nearly continuum spectrum [13]. Aurorae and airglow will be the next most important backgrounds and will include sharp spectral features within the two TEMPO passbands, including atomic lines O (555.7, 630, 636 nm). Na (D lines: 589.0, 589.6 nm) and the excited radical OH* (>500 nm). Aurorae are confined to the polar regions and should be visible to TEMPO at the northernmost reaches of its field of regard. Airglow is more ubiquitous; VIIRS detects atmospheric waves in the upper atmosphere as airglow emission features and can observe reflected airglow from the tops of clouds [14]. Stray light from the sun even if it is >60° from the optical axis when we do our nighttime observing could also produce a background to interfere with retrievals.

We have not yet fully analyzed the impact of these dim background signals on retrievals. The Na D lines in nighttime airglow will correlate well with the spectra of Na-vapor lamps and may cause a spatially smooth retrieved Na lamp signal to be retrieved. We may need to include interfering sources in our spectral library or otherwise model or calibrate their contributions. When spectral fitting residuals are found to exhibit structure, additional modeling will be required.

4.4 Distribution of Nightlights

We can envision the value of the TEMPO retrievals by looking at a VIIRS-DNB clear-sky composite remapped and binned to the TEMPO geometry and resolution. This is shown in Fig. 5, where radiance levels are color coded in levels relevant to the sensitivities shown in Fig. 4. There are many areas where the radiance levels exceed 10 DNB units and typical values in large cities are 100 DNB units or more. The signature of the aurorae is evident in the northernmost part of the field of regard.

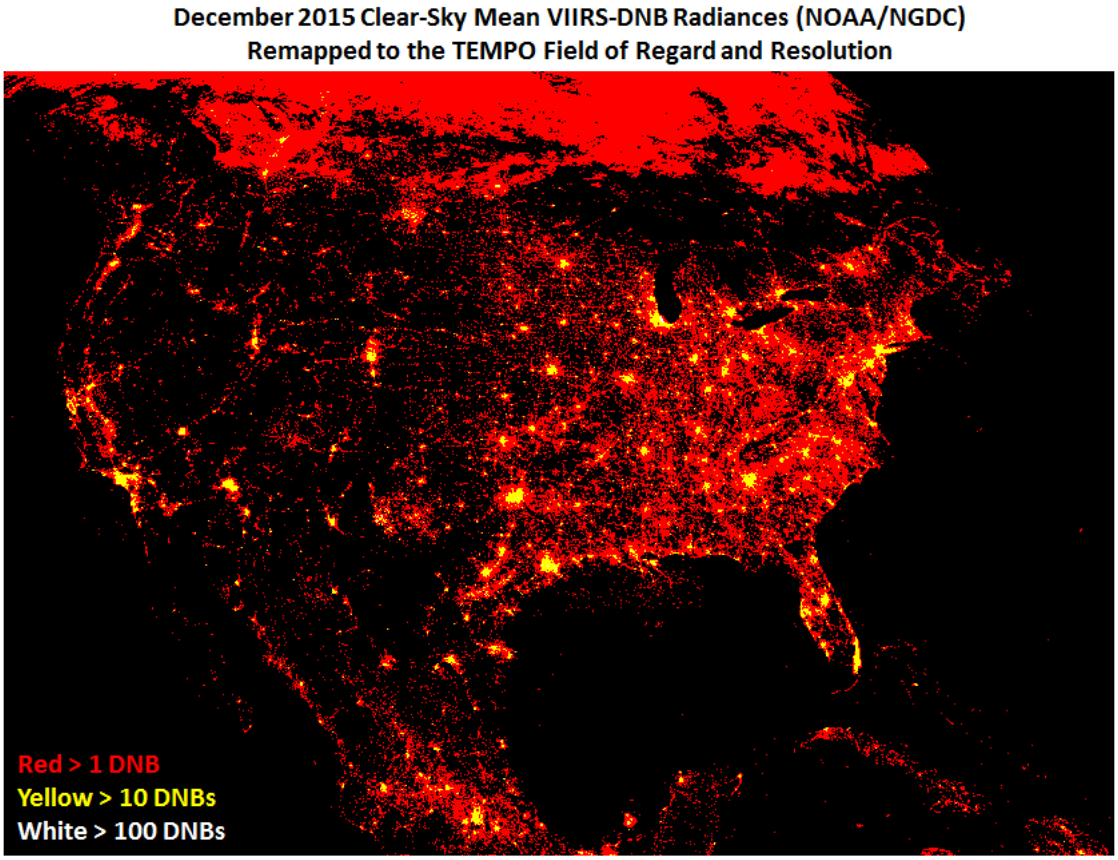

Fig. 5. VIIRS-DNB monthly clear-sky radiances have been remapped and binned to the TEMPO resolution and scan geometry (with TEMPO at 100°W longitude) to represent the TEMPO field of regard. High signal-to-noise retrievals will certainly be possible over major metropolitan areas. Note the evidence of light from the aurorae in this monthly composite.

5. Opportunities for International Collaboration

TEMPO will be part of an international geostationary constellation of spectroscopic instruments primarily for the study of air quality [15]. The Korean Geostationary Environment Monitoring Spectrometer (GEMS) [16] set to launch ~2019 and the European Sentinel-4 [17-18] set to launch ~2022 will cover Asia and Europe respectively from Geostationary Orbit (GEO). In addition, similar air quality missions Sentinel-5p [19] and -5 [20] will cover the Earth from Low-Earth Orbit (LEO) in the 2017 and ~2021 timeframes respectively, providing global coverage but with only one measurement daily per site. GEMS and Sentinel-4 in principle could be operated in a fashion similar to TEMPO at night to broaden the geographic scope of nightlights spectroscopy. However, their spectral coverage is less favorable than that of TEMPO for this purpose. GEMS only covers the wavelengths 300-500 nm and Sentinel-4 covers 305-500 nm and 750-775 nm; both GEMS and Sentinel-4 miss the important spectral structures seen in Fig. 3 between 500-700 nm. A spectrometer in LEO cannot generally dwell as long per pixel as an instrument in GEO, which is a disadvantage for collecting data for nightlights retrievals. Sentinel-5p and -5, moreover, also lack spectral coverage in the 500-675 nm region but do cover 270-495 nm and 270-500 nm respectively. On the other hand, Sentinel-4, -5p, and -5 will all have colder focal planes than TEMPO and GEMS and much lower detector dark currents. Recalling that Poisson noise due to dark current is the dominant noise source for TEMPO nightlights observations, the reduced dark current could be an important mitigating factor to improve the sensitivity for at least those types of lighting radiating in the region from ~300-500nm. Other LEO hyperspectral imagers like the Environmental Mapping and Analysis Program (EnMAP, to be launched in 2017, 420-2450 nm, Guanter et al., 2015) and proposed Hyperspectral InfraRed Imager (HyspIRI, 380 nm-2500 nm, Lee et al., 2015) cover most of the spectral range (~400-900 nm) needed to resolve lighting types shown in Fig. 3 at high spatial resolution (tens to hundreds of meters) but with coarser spectral resolution of ~10 nm, and thus can also provide some capabilities to measure different lighting types. In summary, the capabilities of each spectroscopic instrument must be examined individually considering their dwell time per spatial pixel, spectral coverage, and detector dark current. An instrument in GEO will generally permit longer dwell times per spatial pixel but of course not generally possess the finer spatial resolution of an equivalent LEO instrument.

6. Conclusion

We have shown that TEMPO will provide a powerful new tool to complement VIIRS for the study of nightlights. TEMPO spectral retrievals will map the utilization of artificial lighting by type over North America with good sensitivity. Including VIIRS-DNB data in the retrievals further improves retrieval accuracy for sources lacking sharp spectral features. Other air quality instruments, such as GEMS, Sentinel-4, -5p, and -5 may offer some possibilities for the study of nightlights over other geographic areas but their spectral coverage is apparently less well suited than that of TEMPO to this particular purpose. Nevertheless, we invite our international colleagues to examine these possibilities.

References

[1] Zoogman, P., Liu, X., Suleiman, R. M., Pennington, W. F., Flittner, D. E., Al-Saadi, J. A., Hilton, B. B., Nicks, D. K., Newchurch, M. J., Carr, J. L., Janz, S. J., Andraschko, M. R., Arola, A., Baker, B. D., Canova, B. P., Chan Miller, C., Cohen, R. C., Davis, J. E., Dussault, M. E., Edwards, D. P., Fishman, J., González Abad, G., Grutter, M., Herman, J. R., Houck, J., Jacob, D. J., Joiner, J., Kerridge, B. J., Kim, J., Krotkov, N. A., Lamsal, L., Li, C., Lindfors, A., Martin, R. V., McElroy, C. T., McLinden, C., Natraj, V., Neil, D. O., Nowlan, C. R., O'Sullivan, E. J., Palmer, P. I., Pierce, R. B., Pippin, M. R., Saiz-Lopez, Spurr, R. J. D., Szykman, J. J., Torres, O., Veefkind, J. P., Veihelmanna, B., Wang, H., Wang, J., Wulamu, A., Chance, K. (2017). Tropospheric emissions: monitoring of pollution (TEMPO). Journal of Quantitative Spectroscopy and Radiative Transfer, 186, 17-39.

[2] Kyba, C., Garz, S., Kuechly, H., de Miguel, A. S., Zamorano, J., Fischer, J., & Hölker, F. (2014). High-resolution imagery of Earth at night: new sources, opportunities and challenges. Remote sensing, 7(1), 1-23.

[3] Elvidge, C. D., Baugh, K. E., Zhizhin, M., & Hsu, F. C. (2013). Why VIIRS data are superior to DMSP for mapping nighttime lights. Proceedings of the Asia-Pacific Advanced Network, 35, 62-69.

[4] Huang, Q., Yang, X., Gao, B., Yang, Y., & Zhao, Y. (2014). Application of DMSP/OLS nighttime light images: A meta-analysis and a systematic literature review. Remote Sensing, 6(8), 6844-6866.

[5] Falchi, F., Cinzano, P., Duriscoe, D., Kyba, C. C., Elvidge, C. D., Baugh, K., ... & Furgoni, R. (2016). The new world atlas of artificial night sky brightness. Science advances, 2(6), e1600377.

[6] Cinzano, P., Falchi, F., & Elvidge, C. D. (2001). The first world atlas of the artificial night sky brightness. Monthly Notices of the Royal Astronomical Society, 328(3), 689-707.
[7] American Medical Association House of Delegates Annual Meeting 2012. Council on Science and Public Health Report 4, Light pollution: adverse health effects of nighttime lighting. Chicago, Illinois.
[8] Sánchez de Miguel, A., Castaño, J. G., Zamorano, J., Pascual, S., Ángeles, M., Cayuela, L., Martinez, G. M., Challupner, P., Kyba, C. C. M. (2014). Atlas of astronaut photos of earth at night. Astronomy and Geophysics, 55(4) ,4.36.
[9] Laboratory spectra. NOAA: National Center for Environmental Information. Retrieved January 20, 2017. from: http://www.ngdc.noaa.gov/eog/night_sat/spectra.html
[10] Elvidge, C. D., Keith, D. M., Tuttle, B. T., & Baugh, K. E. (2010). Spectral identification of lighting type and character. Sensors, 10(4), 3961-3988.
[11] Liao, L. B., Weiss, S., Mills, S., & Hauss, B. (2013). Suomi NPP VIIRS day-night band on-orbit performance. Journal of Geophysical Research: Atmospheres, 118(22).
[12] Miller, S. D., Mills, S. P., Elvidge, C. D., Lindsey, D. T., Lee, T. F., & Hawkins, J. D. (2012). Suomi satellite brings to light a unique frontier of nighttime environmental sensing capabilities. Proceedings of the National Academy of Sciences, 109(39), 15706-15711.
[13] Kieffer, H. H., & Stone, T. C. (2005). The spectral irradiance of the Moon. The Astronomical Journal, 129(6), 2887.
[14] Miller, S. D., Straka, W. C., Yue, J., Smith, S. M., Alexander, M. J., Hoffmann, L., ... & Partain, P. T. (2015). Upper atmospheric gravity wave details revealed in nightglow satellite imagery. Proceedings of the National Academy of Sciences, 112(49), E6728-E6735.
[15] CEOS Atmospheric Composition Constellation (ACC). (2011). A Geostationary Satellite Constellation for Observing Global Air Quality: An International Path Forward. Retrieved January 20, 2017. from http://ceos.org/document_management/Virtual_Constellations/ACC/Documents/ACC_White-Paper-A-Geostationary-Satellite-Cx-for-Observing-Global-AQ-v4_Apr2011.pdf.
[16] Kim, J. (2012, April). GEMS (Geostationary Environment Monitoring Spectrometer) onboard the GeoKOMPSAT to monitor air quality in high temporal and spatial resolution
[17] Ahlers, B., Courrèges-Lacoste, G. B., Guldimann, B., Veihelmann, B., Stark, H., & Dobber, M. GMES Sentinel-4/UVN instrument concept and calibration approach. (2011). Proceeding of 20th CALCON Technical Conference, Utah, USA.
[18] Courrèges-Lacoste, G. B., Ahlers, B., Guldimann, B., Short, A., Veihelmann, B., & Stark, H. The Sentinel-4/UVN instrument on-board MTG-S. (2011). Proceedings of 2011 EUMETSAT Meteorological Satellite Conference, Oslo, Norway.
[19] Veefkind, J. P., Aben, I., McMullan, K., Förster, H., De Vries, J., Otter, G., ... & Van Weele, M. (2012). TROPOMI on the ESA Sentinel-5 Precursor: A GMES mission for global observations of the atmospheric composition for climate, air quality and ozone layer applications. Remote Sensing of Environment, 120, 70-83.
[20] Sierk, B., Bezy, J. L., Caron, J., Meynard, R., Veihelmann, B., & Ingmann, P. (2012, October). The GMES Sentinel-5 mission for operational atmospheric monitoring: Status and Developments. In Proceedings of the ICSO (International Conference on Space Optics), Ajaccio, Corse, France, Oct (pp. 9-12).
[21] Guanter, L., Kaufmann, H., Segl, K., Foerster, S., Rogass, C., Chabrillat, S., Kuester, T., Hollstein, A., Rossner, G., Chlebek, C., Straif, C., Fischer, S., Schrader, S., Storch, T., Heiden, U., Mueller, A., Bachmann, M., Mühle, H., Müller, R., Habermeyer, M., Ohndorf, A., Hill, J., Buddenbaum, H., Hostert, P., van der Linden, S., Leitão, P. J., Rabe, A., Doerffer, R., Krasemann, H., Xi, H., Mauser, W., Hank, T., Locherer, M., Rast, M., Staenz, K., Sang, B. (2015). The EnMAP spaceborne imaging spectroscopy mission for earth observation, Remote Sensing. 7 (7), 8830-8857.
[22] Lee, C. M., Cable, M. L., Hook, S. J., Green, R. O., Ustin, S. L., Mandl, D. J., & Middleton, E. M. (2015). An introduction to the NASA Hyperspectral InfraRed Imager (HyspIRI) mission and preparatory activities. Remote Sensing of Environment, 167, 6-19.